JACS
JOURNAL OF THE AMERICAN CHEMICAL SOCIETY
Communication
pubs.acs.org/JACS

# DNA Tetraplexes-Based Toehold Activation for Controllable DNA Strand Displacement Reactions

Wei Tang, Huaming Wang, Dingzhong Wang, Yan Zhao, Na Li, and Feng Liu*

Beijing National Laboratory for Molecular Sciences, Key Laboratory of Bioorganic Chemistry and Molecular Engineering of Ministry of Education, College of Chemistry and Molecular Engineering, Peking University, Beijing 100871, China

Supporting Information

**ABSTRACT:** Most of the dynamic DNA devices are rationally constructed by utilizing toehold-mediated DNA strand displacement reactions. However, such approaches have been mainly limited to the operation with double-stranded hybridization and lack the versatility of DNA scaffold responses for additional levels of controlling DNA strand displacement reactions. Herein, we propose a toehold activation strategy based on the DNA tetraplex (G-quadruplex or i-motif), where the toehold domain is designed by attaching a complementary single-stranded segment (**CS**) to a G-rich/C-rich segment. Modulating G-quartet/C·C$^+$ numbers and/or the **CS** lengths can easily tune the strand displacement kinetics. This scheme allows fine control of DNA strand displacement rates over 2 orders of magnitude by adjusting the concentration of various environmental stimuli. This strategy expands the rule set of designing dynamic DNA devices and will be useful in building diverse environmental stimuli-fuelled molecular devices.

DNA is a powerful and versatile nanoscale material for engineering dynamic nanodevices.[1] Utilizing toehold-mediated DNA strand displacement reactions, a series of dynamic DNA devices, such as nanomachines,[2] logic circuits,[3] and catalytic amplifiers,[4] have been rationally constructed. In general, strand displacement reaction is initiated by hybridization at the toehold domain[1a,5] and can be roughly controlled by varying the toehold binding strength.[6] Recently, engineering control of dynamic DNA devices by programmed sequestration and activation of the toehold, such as blocking or isolating the toehold and activating it by subsequent exposure or connection, has drawn the attention of researchers.[1c,3a,7] However, these strategies have been mainly limited to the operation with double-stranded hybridization and lack the versatility of DNA scaffold responses to develop regulative methods toward the control of strand displacement. As a result, it remains a challenge to create new schemes of toehold sequestration and activation based on higher order DNA scaffolds for additional levels of controlling DNA strand displacement reactions.

In addition to the classical double helix, DNA is also able to form the tetraplexes, such as intermolecular and/or intramolecular G-quadruplex[8] and i-motif[9] structures, which are specifically correlated to a number of environmental stimuli. DNA tetraplex has been an emerging topic in nucleic acid research because of the unique biological function.[10] Furthermore, DNA tetraplex with a higher order structure is regarded as a fascinating material for the DNA nanotechnology.[11] In this work, we develop a novel toehold activation strategy based on the DNA tetraplex (G-quadruplex or i-motif), which can finely control the DNA strand displacement kinetics by regulating various environmental stimuli. This strategy provides additional design flexibility for dynamic DNA devices.

G-quadruplex typically forms from G-rich DNAs and is stabilized by the coordination of specific metal cations which bind between successive G-quartets.[8] We first develop the G-quadruplex-based toehold activation strategy, and the design principle is illustrated in Figure 1A. The substrate DNA ($\mathbf{S_G}$) is partially hybridized with the reporter DNA (**R**) at the branch migration domain (red) to form an $\mathbf{S_G R}$ duplex. A toehold domain, an unpaired overhang on strand $\mathbf{S_G}$ (blue), composes

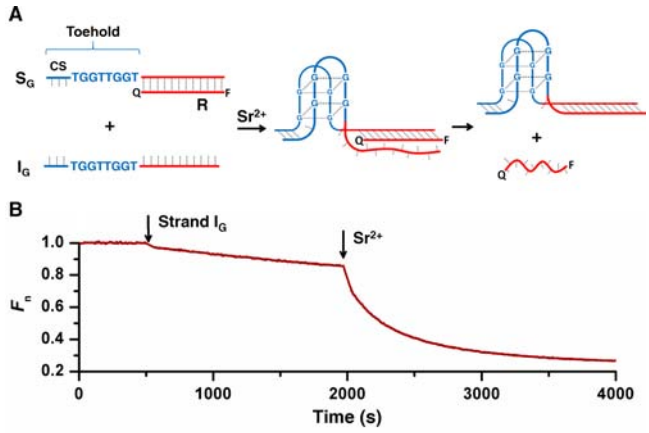


**Figure 1.** (A) Principle of the G-quadruplex-based toehold activation strategy. A toehold domain (blue) is designed by attaching a **CS** to a G-rich segment. $\mathbf{S_G R}$ duplex is formed by prehybridizing strand $\mathbf{S_G}$ and strand **R** (labeled with fluorophore (F) and quencher (Q)). $Sr^{2+}$ ions trigger the formation of G-quadruplex between the toehold and strand $\mathbf{I_G}$, which promotes the following displacement of strand **R**. Displacement reaction is monitored by quenching of fluorescence from strand **R**. The nucleotide sequences of all strands are provided in Table S1−S3. (B) Dynamic control of strand displacement kinetics. Twenty nM strand $\mathbf{I_G}$ and 10 mM $Sr^{2+}$ were added successively into 20 nM $\mathbf{S_G R}$ duplex solution. $F_n$ is the normalized fluorescence intensity (see Text S2).

**Received:** June 17, 2013
**Published:** September 5, 2013

   dx.doi.org/10.1021/ja406053b | J. Am. Chem. Soc. 2013, 135, 13628−13631

of a G-rich segment ($TG_2T_2G_2T$) and a complementary single-stranded segment (**CS**). In invading DNA ($\mathbf{I_G}$), the docking domain (blue) consisted of **CS**, and the same G-rich segment can dock to the toehold by the formation of G-quadruplex in the presence of stabilizer. Thus, a G-quadruplex stabilizer, such as $Sr^{2+}$,[12] is utilized as the toehold activator to further induce the following strand displacement. As shown in Figure 1B, in the absence of $Sr^{2+}$, the G-rich segment is sequestered due to the base pair (G-G and T-T) mismatch, which results an extremely slow strand displacement between the $\mathbf{S_GR}$ duplex and strand $\mathbf{I_G}$ at room temperature. However, when $Sr^{2+}$ is presented, the formation of G-quadruplex promotes the following displacement of strand **R**.

The native polyacrylamide gel electrophoresis (PAGE) experiment (Figure 2A) and the circular dichroism (CD)

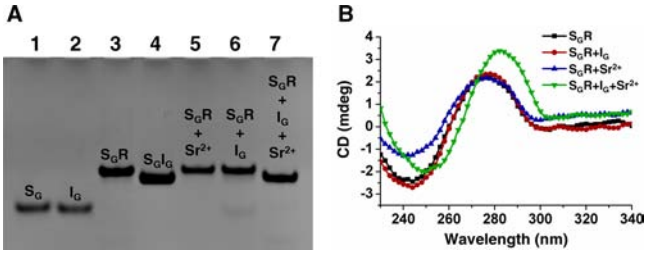


**Figure 2.** Validation of the G-quadruplex-based toehold activation mechanism. (A) Native PAGE (12%) analysis. Lane 1: 2 $\mu$M strand $\mathbf{S_G}$, lane 2: 2 $\mu$M strand $\mathbf{I_G}$, lane 3: 2 $\mu$M $\mathbf{S_GR}$ duplex, lane 4: 2 $\mu$M $\mathbf{S_GI_G}$ duplex, lane 5: 2 $\mu$M $\mathbf{S_GR}$ duplex and 10 mM $Sr^{2+}$, lane 6: 2 $\mu$M $\mathbf{S_GR}$ duplex and 2 $\mu$M strand $\mathbf{I_G}$, lane 7: 2 $\mu$M $\mathbf{S_GR}$ duplex, 2 $\mu$M strand $\mathbf{I_G}$, and 10 mM $Sr^{2+}$. (B) CD spectroscopy analysis for the formation of G-quadruplex. Initial concentrations: 0.5 $\mu$M $\mathbf{S_GR}$ duplex, 0.5 $\mu$M strand $\mathbf{I_G}$, and 10 mM $Sr^{2+}$. All the samples were incubated at room temperature for 30 min.

spectroscopy analysis (Figure 2B) were applied to verify the proposed toehold activation strategy. $Sr^{2+}$ was added to the $\mathbf{S_GR}$ duplex first (lane 5), no obvious change in band shift compared to the $\mathbf{S_GR}$ duplex alone (lane 3) is observed. After adding strand $\mathbf{I_G}$ into the $\mathbf{S_GR}$ duplex (lane 6), a strong band of $\mathbf{S_GR}$ duplex is observed, and the band of $\mathbf{S_GI}$ duplex is almost invisible, indicating that the strand displacement between the $\mathbf{S_GR}$ duplex and strand $\mathbf{I_G}$ is extremely slow. However, adding both strand $\mathbf{I_G}$ and $Sr^{2+}$ to the $\mathbf{S_GR}$ duplex (lane 7), the observed strong band as the same with lane 4 indicates the formation of $\mathbf{S_GI}$ duplex after the release of strand **R** from the $\mathbf{S_GR}$ duplex according to Figure 1A. The CD spectrum of $\mathbf{S_GR}$ duplex has a positive band near 275 nm and a negative band near 245 nm that are characteristic of a Watson−Crick duplex.[13] The addition of strand $\mathbf{I_G}$ or $Sr^{2+}$ does not cause any obvious change in band shift. However, adding both strand $\mathbf{I_G}$ and $Sr^{2+}$ to the $\mathbf{S_GR}$ duplex, a dramatically different CD spectrum with a positive band near 285 nm and a negative band near 250 nm is shown, that can be assigned to antiparallel strand quadruplex structure.[14] Hence, the experiment results confirm the rationality of the proposed toehold activation strategy.

To explore the effect of the G-quartet numbers and the **CS** lengths on the strand displacement rate, three most studied G-rich segments, ($TG_2T_2G_2T$), ($TG_3T_2AG_3T$), and ($TG_4T_4G_4T$), which can form stable intermolecular quadruplexes in the presence of $Sr^{2+}$,[8b,c] were used in the design of toeholds. The corresponding G-quadruplexes compose of two, three, and four G-quartets (denoted G2, G3, and G4), respectively. As shown in Figure 3A, very slow strand displacements are observed for

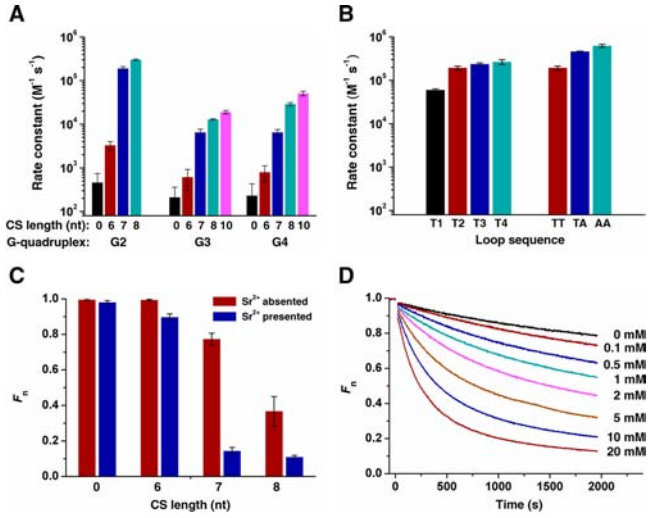


**Figure 3.** (A) Effect of the G-quartet numbers and the **CS** lengths on the strand displacement rate. (B) Effect of the loop region with various lengths and sequences on the strand displacement rate. (C) Effect of the **CS** lengths (Figure S1) on the fluorescent discrimination of G2 system in the absence or presence of $Sr^{2+}$ at 30 min. Initial concentrations (A−C): 20 nM $\mathbf{S_GR}$ duplex, 20 nM strand $\mathbf{I_G}$ (Figure S2), and 20 mM $Sr^{2+}$. The error bars represent the standard deviation of three measurements. (D) Effect of the concentrations of $Sr^{2+}$ on the strand displacement kinetics (**CS** = 7). In a typical experiment, the $\mathbf{S_GR}$ duplex (1 mL, 20 nM) was placed in a cuvette, and then both strand $\mathbf{I_G}$ (1 $\mu$L, 20 $\mu$M) and $Sr^{2+}$ (2 $\mu$L at the proper concentration) were added and mixed quickly within 30 s to initiate the reaction. The reaction rate depends strongly on the concentration of the invading strand (Figure S3), indicating that the second-order toehold association contributes significantly to the overall reaction rate. Thus, all the rate constants were calculated according to Text S2.

all the systems without the **CS**, indicating that the stability of formed G-quadruplexes by themselves is not strong enough to efficiently promote the following strand displacements in our systems.[8d] While the **CS** lengths were increased from 6 to 10, the strand displacement rates can be tuned over 2−3 orders of magnitude. Furthermore, comparing the reaction rates of three G-quadruplex systems with the same **CS** length, the stability order is G2 > G4 > G3 for the "chair" type.[8e] The research results show that the strand displacement rates can be regulated by modulating the G-quartet numbers and/or the **CS** lengths.

The G2 system was chosen to study the effect of the loop region in G-quadruplex on the strand displacement rate. One to four thymines were designed as the loop sequences, denoted T1, T2, T3, and T4, respectively. As shown in Figure 3B, a relatively slower strand displacement is observed for T1 system, which could be resulted from the steric hindrance of the loop in the "chair" type G-quadruplex.[8e] While for T2−T4 systems, the reaction rates are no obvious change. Furthermore, with the loop sequence design of (TT) in strand $\mathbf{S_G}$ and (TT), (TA), or (AA) in strand $\mathbf{I_G}$ respectively, the reaction rates are increased from $1.9 \times 10^5$ to $6.3 \times 10^5$ $M^{-1}$ $s^{-1}$, with the number of matched base pairs rising from 0 to 2 (Figure 3B). The above results suggest that the more stable loop structure can promote the strand displacement rate.

We further investigated the effect of $Sr^{2+}$ on the strand displacement rate. In the absence or presence of $Sr^{2+}$, the


dx.doi.org/10.1021/ja406053b | J. Am. Chem. Soc. 2013, 135, 13628−13631

fluorescence signal can be regulated over a wider range (63%) for 7 nt **CS** length than that of 0 nt (2%), 6 nt (10%), and 8 nt (26%) **CS** length (Figure 3C), indicating that the toehold with a 7 nt **CS** presents the largest fluorescent discrimination for $Sr^{2+}$. As shown in Figure 3D, the strand displacement rates can be accelerated in a $Sr^{2+}$ concentration-dependent way. When $Sr^{2+}$ concentrations are increased from 0 to 20 mM, the rate constants can be regulated in the range from $6.3 \times 10^3$ to $2.0 \times 10^5$ $M^{-1}$ $s^{-1}$. The strand displacement reaction also shows a high selectivity for $Sr^{2+}$ (Figure S4), due to the stronger effect of $Sr^{2+}$ on the stability of G-quadruplex than that of $K^+$, $Na^+$, $Mg^{2+}$, and $NH_4^+$ ions.[14,15] Therefore, it is proved that the presence of $Sr^{2+}$ can effectively modulate the G-quadruplex-based toehold strength, and the strand displacement kinetics can be finely adjusted by varying the concentrations of $Sr^{2+}$.

To demonstrate the general applicability of G-quadruplex-based toehold activation strategy, we adapted the system to a clinically relevant input, adenosine triphosphate (ATP). The anti-ATP aptamer forms a G-quadruplex nanostructure that consists of two stacked G-quartets upon its binding to ATP.[16] The anti-ATP aptamer was split into two fragments: one fragment was designed in the toehold and the other was included in strand $\mathbf{I_A}$ (Figure S5). In the presence of ATP, the toehold and strand $\mathbf{I_A}$ would assemble to form intact structures by binding ATP that promotes the following strand displacement (Figure S6). The native PAGE experiment and CD spectroscopy analysis confirm the rationality of this toehold activation strategy (Figures S7 and S8). We also proved that the strand displacement kinetics can be finely controlled by varying the concentrations of ATP. At a fixed concentration of 20 nM $\mathbf{S_AR}$ duplex and 100 nM strand $\mathbf{I_A}$ (Figure S9) with 4 nt **CS** length (Figure S10), the rate constants can be regulated in the range from $3.7 \times 10^2$ to $3.2 \times 10^4$ $M^{-1}$ $s^{-1}$ when ATP concentrations were increased from 0 to 2 mM (Figure S11). The strand displacement kinetics also shows a high selectivity for ATP (Figure S12). These results demonstrate an application of the G-quarduplex-based toehold activation for controllable DNA strand displacement reaction by ATP. This G-quadruplex-based toehold activation strategy can be extended to couple with other ligands specifically binding with G-rich sequences. Together using this strategy, the dynamic DNA devices with the higher order structures can be feasibly constructed, which is fuelled by G-quadruplex correlated environmental stimuli.

Comparing with G-quadruplex, a cytidine-rich oligomer forms a radically different DNA tetraplex, which is known as i-motif.[9] We also propose the i-motif-based toehold activation strategy as illustrated in Figure 4A. The toehold domain, an unpaired overhang on strand $\mathbf{S_C}$ (blue), composes of a C-rich segment ($C_4TA_2C_4$) and a **CS**. In invading DNA ($\mathbf{I_C}$), the docking domain (blue) consisted of **CS**, and the same C-rich segment can dock to the toehold by the formation of i-motif in slightly acidic solutions. In closely neutral solutions, the toehold is sequestered due to the base pair (C-C and A-A) mismatch, which results an extremely slow strand displacement. When pH value is lowered, the cytosines become partially protonated, leading to the formation of i-motif between the toehold and the docking domain that accelerates the following strand displacement. The native PAGE experiment and CD spectroscopy analysis confirm that this sequestered toehold can be activated by adjusting pH values (Figures S13 and S14). We studied various number of $C{\cdot}C^+$ pairs applied for i-motif-based toehold activation. The research results of four, six, and eight $C{\cdot}C^+$ pair

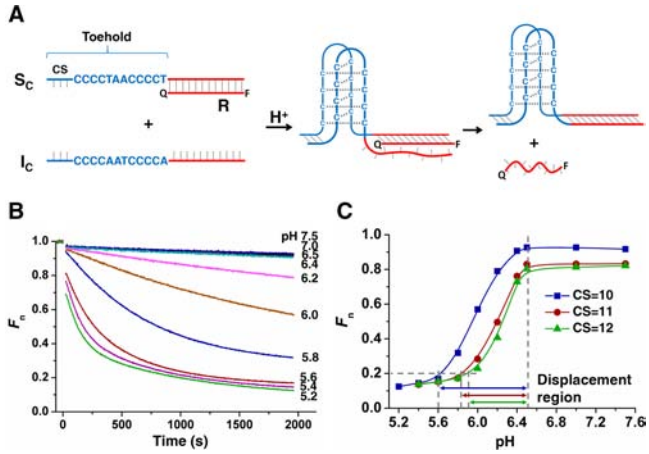


**Figure 4.** (A) Principle of the i-motif-based toehold activation strategy. The C-rich segments are designed in the toehold (blue) on strand $\mathbf{S_C}$ and the docking domain (blue) on strand $\mathbf{I_C}$, respectively. In slightly acidic solutions, the cytosines become partially protonated, leading to the formation of i-motif between the toehold and the docking domains, which accelerates the following displacement of strand **R**. Displacement is monitored by quenching of fluorescence from strand **R**. (B) Effect of the pH values on the strand displacement kinetics. In a typical experiment, the $\mathbf{S_CR}$ duplex (1 mL, 20 nM) in buffer solution with various pH values was placed in a cuvette, and strand $\mathbf{I_C}$ (5 $\mu$L, 20 $\mu$M) was added and mixed quickly within 30 s to initiate the reaction. (C) Estimation of the efficiency of the pH for regulated strand displacement reactions with various **CS** length at 30 min. The reaction mixture contained 20 nM $\mathbf{S_CR}$ duplex and 100 nM strand $\mathbf{I_C}$.

systems indicate that the strand displacement rates can be tuned by modulating the number of $C{\cdot}C^+$ pairs and/or the **CS** lengths (Figure S15).

We also investigated the effect of the solution acidity on the strand displacement kinetics. As shown in Figure 4B, at a fixed concentration of 20 nM $\mathbf{S_CR}$ duplex and 100 nM strand $\mathbf{I_C}$ (Figure S16), the strand displacement rates can be regulated in the range from $3.1 \times 10^2$ to $5.3 \times 10^4$ $M^{-1}$ $s^{-1}$ with reducing pH from 7.5 to 5.2. Moreover, the different displacement regions are observed for 10, 11, and 12 nt **CS** length (Figure 4C), respectively. These results evidence the pH-responsive toehold activation based on the formation of i-motif, and the DNA strand displacement kinetics can be finely controlled by tuning the solution acidity. Thus, by utilizing this strategy, the proton-fuelled dynamic DNA devices with the higher order structures can be feasibly constructed.

In conclusion, we demonstrated a new toehold activation strategy based on the DNA tetraplex (G-quadruplex or i-motif) for additional levels of controlling DNA strand displacement reactions. The crucial element of developed toehold activation strategy is that the designed toehold is sequestered by the base pair mismatch and subsequently activated by the formation of G-quadruplex or i-motif through adjusting environmental stimuli, such as $Sr^{2+}$, ATP, or pH. Thus, the DNA tetraplex-based toehold activation strategy allows the fine control of strand displacement kinetics by adjusting the concentration of various environmental stimuli. The new scheme of toehold activation provides additional design flexibility for dynamic DNA devices involving DNA tetraplexes, which could expand the architecture of dynamic DNA nanotechnology. We anticipate that our strategy can also be applied to construct diverse environmental stimuli-fuelled DNA nanodevices, which may provide a means for biosensing in biological systems.


dx.doi.org/10.1021/ja406053b | J. Am. Chem. Soc. 2013, 135, 13628−13631

## ■ ASSOCIATED CONTENT

### Supporting Information

Supporting figures, DNA sequences, and detailed experimental methods. This material is available free of charge via the Internet at http://pubs.acs.org.

## ■ AUTHOR INFORMATION


### Corresponding Author

liufeng@pku.edu.cn


### Notes

The authors declare no competing financial interest.

## ■ ACKNOWLEDGMENTS

This work was financially supported by the National Natural Science Foundation of China (21035005, 21275013, and 20975006). We thank Prof. Gu Yuan and Wei Tan of Peking University for obtaining the circular dichroism spectra.

## ■ REFERENCES


(1) (a) Yurke, B.; Turberfield, A. J.; Mills, A. P.; Simmel, F. C.; Neumann, J. L. *Nature* **2000**, *406*, 605. (b) Bath, J.; Turberfield, A. J. *Nat. Nanotechnol.* **2007**, *2*, 275. (c) Yin, P.; Choi, H. M. T.; Calvert, C. R.; Pierce, N. A. *Nature* **2008**, *451*, 318. (d) Liu, H.; Liu, D. *Chem. Commun.* **2009**, 2625. (e) Zhang, D. Y.; Seelig, G. *Nat. Chem.* **2011**, *3*, 103. (f) Krishnan, Y.; Simmel, F. C. *Angew. Chem., Int. Ed.* **2011**, *50*, 3124. (g) Liao, S.; Seeman, N. C. *Science* **2004**, *306*, 2072.

(2) (a) Li, J. J.; Tan, W. *Nano Lett.* **2002**, *2*, 315. (b) Shin, J. S.; Pierce, N. A. *J. Am. Chem. Soc.* **2004**, *126*, 10834. (c) Sherman, W. B.; Seeman, N. C. *Nano Lett.* **2004**, *4*, 1203. (d) Green, S. J.; Bath, J.; Turberfield, A. J. *Phys. Rev. Lett.* **2008**, *101*, 238101. (e) Bath, J.; Green, S. J.; Allen, K. E.; Turberfield, A. J. *Small* **2009**, *5*, 1513. (f) Omabegho, T.; Sha, R.; Seeman, N. C. *Science* **2009**, *324*, 67. (g) Modi, S.; Swetha, M. G.; Goswami, D.; Gupta, G. D.; Mayor, S.; Krishnan, Y. *Nat. Nanotechnol.* **2009**, *4*, 325.

(3) (a) Seelig, G.; Soloveichik, D.; Zhang, D. Y.; Winfree, E. *Science* **2006**, *314*, 1585. (b) Frezza, B. M.; Cockroft, S. L.; Ghadiri, M. R. *J. Am. Chem. Soc.* **2007**, *129*, 14875. (c) Qian, L.; Winfree, E. *Science* **2011**, *332*, 1196. (d) Voelcker, N. H.; Guckian, K. M.; Saghatelian, A.; Ghadiri, M. R. *Small* **2008**, *4*, 427.

(4) (a) Dirks, R. M.; Pierce, N. A. *Proc. Natl. Acad. Sci. U.S.A.* **2004**, *101*, 15275. (b) Bois, J. S.; Venkataraman, S.; Choi, H. M. T.; Spakowitz, A. J.; Wang, Z. G.; Pierce, N. A. *Nucleic Acids Res.* **2005**, *33*, 4090. (c) Seelig, G.; Yurke, B.; Winfree, E. *J. Am. Chem. Soc.* **2006**, *128*, 12211. (d) Zhang, D. Y.; Turberfield, A. J.; Yurke, B.; Winfree, E. *Science* **2007**, *318*, 1121. (e) Zhang, D. Y.; Winfree, E. *J. Am. Chem. Soc.* **2008**, *130*, 13921. (f) Li, B.; Ellington, A. D.; Chen, X. *Nucleic Acids Res.* **2011**, *39*, e110. (g) Li, B.; Jiang, Y.; Chen, X.; Ellington, A. D. *J. Am. Chem. Soc.* **2012**, *134*, 13918.

(5) Turberfield, A. J.; Mitchell, J. C.; Yurke, B.; Mills, A. P.; Blakey, M. I.; Simmel, F. C. *Phys. Rev. Lett.* **2003**, *90*, 118102.

(6) (a) Yurke, B.; Mills, A. P. *Genet. Program. Evol. Mach.* **2003**, *4*, 111. (b) Zhang, D. Y.; Winfree, E. *J. Am. Chem. Soc.* **2009**, *131*, 17303. (c) Li, Q.; Luan, G.; Guo, Q.; Liang, J. *Nucleic Acids Res.* **2002**, *30*, e5.

(7) (a) Green, S. J.; Lubrich, D.; Turberfield, A. J. *Biophys. J.* **2006**, *91*, 2966. (b) Genot, A. J.; Zhang, D. Y.; Bath, J.; Turberfield, A. J. *J. Am. Chem. Soc.* **2011**, *133*, 2177. (c) Xing, Y.; Yang, Z.; Liu, D. *Angew. Chem., Int. Ed.* **2011**, *50*, 11934. (d) Chen, X. *J. Am. Chem. Soc.* **2012**, *134*, 263.

(8) (a) Williamson, J. R. *Annu. Rev. Biophys. Biomol. Struct.* **1994**, *23*, 703. (b) Wellinger, R. J.; Sen, D. *Eur. J. Cancer* **1997**, *33*, 735. (c) Haq, I.; Trent, J. O.; Chowdhry, B. Z.; Jenkins, T. C. *J. Am. Chem. Soc.* **1999**, *121*, 1768. (d) Freeman, R.; Liu, X.; Willner, I. *J. Am. Chem. Soc.* **2011**, *133*, 11597. (e) Marathias, V. M.; Bolton, P. H. *Biochemistry* **1999**, *38*, 4355.

(9) Gehring, K.; Leroy, J. L.; Guèron, M. *Nature* **1993**, *363*, 561.

(10) (a) Rankin, S.; Reszka, A. P.; Huppert, J.; Zloh, M.; Parkinson, G. N.; Todd, A. K.; Ladame, S.; Balasubramanian, S.; Neidle, S. *J. Am. Chem. Soc.* **2005**, *127*, 10584. (b) Ahmed, S.; Kintanar, A.; Henderson, E. *Nat. Struct. Biol.* **1994**, *1*, 83. (c) Brooks, T. A.; Hurley, L. H. *Nat. Rev. Cancer* **2009**, *9*, 849. (d) Chen, Y.; Qu, K.; Zhao, C.; Wu, L.; Ren, J.; Wang, J.; Qu, X. *Nat. Commun.* **2012**, *3*, 1074. (e) Biffi, G.; Tannahill, D.; McCafferty, J.; Balasubramanian, S. *Nat. Chem.* **2013**, *5*, 182.

(11) (a) Xu, Y.; Hirao, Y.; Nishimura, Y.; Sugiyama, H. *Bioorgan. Med. Chem.* **2007**, *15*, 1275. (b) Wang, C.; Huang, Z.; Lin, Y.; Ren, J.; Qu, X. *Adv. Mater.* **2010**, *22*, 2792. (c) Yang, Y.; Liu, G.; Liu, H.; Li, D.; Fan, C.; Liu, D. *Nano Lett.* **2010**, *10*, 1393. (d) Modi, S.; Swetha, M. G.; Goswami, D.; Gupta, G. D.; Mayor, S.; Krishnan, Y. *Nat. Nanotechnol.* **2009**, *4*, 325. (e) Alberti, P.; Bourdoncle, A.; Saccà, B.; Lacroix, L.; Mergny, J. L. *Org. Biomol. Chem.* **2006**, *4*, 3383.

(12) Chen, F. M. *Biochemistry* **1992**, *31*, 3769.

(13) (a) Rajendran, A.; Nair, B. U. *Biochim. Biophys. Acta* **2006**, *1760*, 1794. (b) Huang, Y. C.; Sen, D. *J. Am. Chem. Soc.* **2010**, *132*, 2663.

(14) Włodarczyk, A.; Grzybowski, P.; Patkowski, A.; Dobek, A. *J. Phys. Chem. B* **2005**, *109*, 3594.

(15) Kankia, B. I.; Marky, L. A. *J. Am. Chem. Soc.* **2001**, *123*, 10799.

(16) Huizenga, D. E.; Szostak, J. W. *Biochemistry* **1995**, *34*, 656.